ASSESSMENT OF RISKY CORNERING ON A HORIZONTAL ROAD CURVE BY IMPROVING VEHICLE SUSPENSION PERFORMANCE

VIDAS ŽURAULIS[*], VYTENIS SURBLYS

Faculty of Transport Engineering, Vilnius Gediminas Technical University, Vilnius, Lithuania

Abstract. Vehicle stability during cornering on horizontal road curves is a risky stage of travel because of additional factors acting. The main stability factor is centrifugal force, which depends on road curve sharpness and is very sensitive to driving speed usually controlled by the driver. However, the counterforce is produced at tire-road interaction, where different pavement types and states cause a wide variation of tire contact forces and vehicle stability. In the paper, the part of vehicle suspension performance while moving on a sharp horizontal road curve with different levels of pavement roughness was simulated by 14 degrees of freedom vehicle model. The model was built in MATLAB/Simulink software with available pavement roughness selection according to ISO 8608. The influence of variable suspension damping available in modern vehicles on risky cornering is analysed when a vehicle reaches the edge of the pavement with its specific roughness. Critical parameters of vehicle stability depending on road curvature, pavement roughness and driving speed are selected to assess the solutions for safe cornering.

Keywords: horizontal curve, edge of pavement, road roughness, critical speed, vehicle stability, vehicle suspension, damping force.

* Corresponding author. E-mail: vidas.zuraulis@vilniustech.lt

Vidas ŽURAULIS (ORCID ID 0000-0002-6210-7642)
Vytenis SURBLYS (ORCID ID 0000-0001-6363-0593)

Introduction

In the transport sector, safety affects the number of road deaths. In the European Union, 31 500 people died on the roads in 2010, 26 000 in 2013, 25 250 in 2017 (Schiehlen & Iroz, 2015; 12th Annual..., 2018). However, despite the progress, 1.35 million people die in road accidents each year (World Health Organization, 2018). Moreover, a target to halve the number of road fatalities by 2020, with respect to 2010 (European Commission, 2010), has not been successfully implemented over the past five years.

In 2018, 57.5% of road fatalities in European motorways and rural roads were related to motor vehicles, excluding motorcycles (European Commission, 2018). An overview of accidents related to horizontal curves in different countries for the last two decades is shown in Table 1. Despite various data contexts, it is evident that the accident rate at horizontal road curves is still relatively high for all regions. Higher risk on horizontal road curves is also identified and highlighted in road design and safety manuals (AASTHO, 2010; PIARC, 2003). Moreover, timely maintenance along with road design considering safety has a significant impact on accident risk reduction.

Analysing the risk of driving and overtaking on road curves, Swedish researchers found that left curves were sensitive to road superelevation and right curves – to its radius (Othman et al., 2010). The field test with 32 participants showed different drivers' behaviour depending on a curve direction where the speed was higher on the right curve than on the left one. The study was conducted because of the observed higher accident rate on the right curves than on the left ones in Swedish reports. Other driving-based research at curved road sections showed that the fluctuations of driving trajectories increased with an increasing radius of the road curve (Xu et al., 2018). It was found that the vehicle encroached the oncoming lane during curve cutting and overcorrection when drivers had to steer back to correct the lateral location of the vehicle. The study covered three groups of radii: 10–50 m, 50–200 m, and 100–200 m.

The research of horizontal curves within the secondary roads of road network in the Czech Republic showed that the radius of 50–200 m was the most frequent one (Bíl et al., 2018). Slightly more than 40% of horizontal curves on the secondary roads had their radius lower than 200 m. The research of measurement technology of curve radius showed that driver's faults in safety performance estimation increased for low radius and length curves (Bogenreif et al., 2012). Another analysis of risky curves of the Czech road network showed that at least one hazardous horizontal curve occurred at 10% country roads (Bíl et al., 2019).

Table 1. Overview of accidents related to horizontal
road curves in different countries

Accidents related with road curve	Location	Data context	Reference
25–30%	–	Part of all road fatalities	Lamm et al., 1999
30%	Australia	Part of all road crashes	Shields et al., 2001
87%	United States	Run-off-road and head-on crashes; part of all fatal crashes at horizontal curves	Torbic et al., 2004
76%		Single-vehicle crashes in which the vehicle left the road and hit a fixed object or overturned; part of all fatal crashes at horizontal curves	
63.44%	Queensland, Australia	Part of all fatalities in rural roads	Queensland Transport, 2006
25.17%		Part of all fatalities in rural roads required hospitalisation	
42%	United States	Part of all lane departure crashes	AASHTO, 2008
1.5× – 4×	–	Times greater accident rate than at straight road sections	Aram, 2010
21%	North Carolina, U.S.	Part of collisions at curves on two-lane roads (2003–2005)	Hummer et al., 2010
14%		Part of collisions at curves on all roads (2003–2005)	
40%	West Europe	Part of run-off-road crashes when single vehicles are involved	SafetyNet, 2010
10%	Europe	Part of all single-vehicle or run-off-road accidents	ERA-NET ROAD, 2012
45%		Part of all single-vehicle or run-off-road fatal accidents	
25%	United States	Part of all fatal crashes occurring on horizontal road curves	Federal Highway Administration, 2014
22%	–	Part of road departure crashes without loss of control	Mastinu & Ploechl, 2014
39%	Australia	Part of fatal crashes (2008–2009)	Rakotonirainy et al., 2015
13%	Spain	Part of all road fatalities	Dirección General de Tráfico, 2015

Table 1. Overview of accidents related to horizontal
road curves in different countries

Accidents related with road curve	Location	Data context		Reference
60–70%	–	Part of single-vehicle run-off-the-road accidents of all fatal crashes		Calvi, 2015
35%	Croatia	Part of total accidents with fatalities occurred along horizontal curves		Maljković & Cvitanić, 2016
45.2%	Czech Republic	Part of all road accidents in secondary roads		Bíl et al., 2018
22.6%	Czech Republic	Part of all horizontal road curves with at least one road accident		Bíl et al., 2019
13%	Lithuania	Part of all fatal road accidents (2015–2019)		Lithuanian Road Police, 2020
8%	Italy	Part of all road accidents between two vehicles		Eboli et al. 2020
71%	Norway	Part of all crashes that occurred in curves caused by speeding and driving under the influence of alcohol	single-vehicle crashes	Høye, 2020
46%			other crashes	
23.1%	–	Extremely severe crashes occurred on the downgrade horizontal curve segments		Xu et al., 2020

The occurrence of road accident of vehicle departing from the roadway by the rollover of vehicle wheels entering the slope was investigated using computer simulation (Cheng et al., 2020). Utilising software of road accident investigation PC-Crash, the speed was identified as the most important risk factor for accidents comparing with others (in terms of significance): longitudinal slope, hard shoulder width, adhesion coefficient, and horizontal curve radius. The correlation model confirmed that the combination of a vehicle speed with a horizontal curve radius had the most considerable impact of interaction on a road accident. Another driving simulation-based research revealed a significant difference among incident probabilities depending on a discrepancy between driver's perceived speed and maximum safe speeds at road curves of 200 and 300 m radius (Yotsutsuji et al., 2017). Road safety measures as warning signs with road surface markings before the curves were considered effective to reduce speeding accidents, but were not treated as a long-term solution.

The significant difference of 17–98% of cases when drivers tended to exceed posted speed limit was determined after speed measurement in a

Vidas Žuraulis,
Vytenis Surblys

Assessment
of Risky Cornering
on a Horizontal Road
Curve by Improving
Vehicle Suspension
Performance

specific section of Lithuania's regional roads with ten horizontal curves (Šeporaitis et al., 2020). The lowest curve radius of 60 m with 70 km/h posted speed was involved in that research, while the largest radius of 550 m was with 90 km/h posted speed. The authors emphasise the problem of difference between road design guidelines and permissible speed. A faulty driver's expectation about safe speed from road geometry was also noted.

Gooch et al. (2016) identified that drivers kept a lower speed at road sections with the sequence of sharp curves. The uncertainty of the next curve induces the awareness of potential risk. The same tendency of lower risk at adjacent sharp curves with a shorter distance between curves was summarised by Elvik (2019). However, the same author, in his previous study, evaluated the data from ten countries, which showed a significant increase in the accident rate at curves with lower than 300 m radius (Elvik, 2013). The matter analysis was for single road curves.

On road sections with intensive changes of the trajectory (R < 200 m), various defects of the pavement caused by the increased wheel loads are more frequently met, so driving on such road sections is more risky. A number of vehicle active safety systems as Electronic Stability Program (ESP), Lane Departure Warning / Keeping (LDW / LDK), Curve Speed Warning (CSW), Adaptive Front Lighting (AFL) and others are attributed as accident-preventing ones at road curves (Furlan et al., 2020). However, vehicle–road interaction is most important for cornering stability, which is firstly ensured by the highest possible wheel normal load and better tire grip, as a result.

The present paper discusses the wear of road pavement edge and its impact on the vehicle controllability in critical situations on horizontal road curve. A relatively new approach to keep the driving safety level is analysed by suggesting a specific design of semi-active suspension as a measure for reducing the loss of the vehicle stability on a single road curve with pavement defects. The described particular suspension tuning and road conditions make the research comprehensive and familiar for both road infrastructure and vehicle design specialists. The first section analyses the pavement wear and the appeared defects as well as the methods for their establishment. In the second section, the principal factors that affect the vehicle movement on a damaged pavement are reviewed from the perspective of the impact of the tire adhesion and the vehicle suspension. In the third section, a theoretical investigation of a vehicle movement with different characteristics of the suspension on road curves is described, and its results are provided. At the end of the paper, conclusions are drawn and plans for future research are presented.

# 1. Road surface deterioration

On their use, roads are influenced by various natural conditions, such as climatic, topographic, hydrological, relief and geological conditions as well as the surrounding flora. The most important are the following climatic conditions to be assessed on designing motorways: precipitation and its distribution between months, the annual temperature regime, the snow cover formation regime, the wind speed and direction, the depth of the frozen ground, the temperature of the surface of the pavement, the conditions for moisture evaporation (Leonovič et al., 2013).

Causes of pavement damage are influenced by vehicle loads, the climate, temperature or relief (Canestrari et al., 2020). The main types of pavement distress are cracking, patching and potholes, surface deformation, surface defects, and miscellaneous distress (Miller & Bellinger, 2014). This investigation focuses on the impact of pavement damage, especially edge cracking, on driving stability (Fig. 1). The issue is recognised mostly in secondary roads with horizontal curves.

The problem of edge cracking is particularly topical in cold and warm climate zones (Ahmad & Khawaja, 2018; Shuler & Nobe, 2007). Cracks become particularly abundant if water penetrates into the underlying
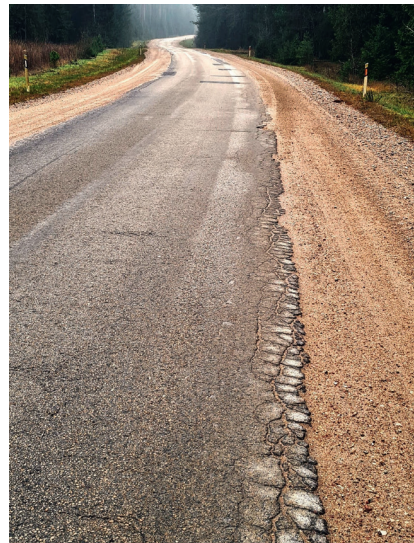
a)   b)

Figure 1. Risky horizontal road curves on the pavement with edge cracking (authors' photographs)

Vidas Žuraulis,
Vytenis Surblys

Assessment
of Risky Cornering
on a Horizontal Road
Curve by Improving
Vehicle Suspension
Performance

layer of the pavement through the primary crack. Thus, the layer under the asphalt pavement becomes softer. In addition, an increased load on the vehicle wheels driving close to the pavement edge provides an impact as well. This takes place when the pavement is narrow, in particular on regional roads and highways. An insufficient road asphalt layer also affects the vulnerability of the road pavement because the pavement is more rapidly damaged by abundant vehicles. Temperature fluctuations in spring and autumn, snow and ice induce the damage of the pavement edges.

The unevenness of road pavement is one of the principal road quality indicators (Sivilevičius et al., 2017) that affect traffic safety and driving comfort. In general, it depends on unevenness level and the number and size of pavement defects (potholes, patches, transverse, longitudinal and meshy cracks, waves etc.) (Paukštė, 2015). An International Roughness Index (IRI) is used to describe road unevenness (Sivilevičius & Vansauskas, 2013; Múčka, 2019; Pawar et al., 2018; ASTM E1926-08, 2015). The minimum value of IRI is for airport runways and new highways where the design speed is higher than 100 km/h, while the maximum value of IRI is typical of rough and unpaved roads.

An International Road Assessment Programme (iRAP) from 54 countries showed that 44% of vehicles assessed travel on roads by one or two stars of the five possible (World Health Organization, 2018). The same report highlights that 124 countries (mostly low- and middleincome) apply only one or even none of the United Nations (UN) safety standards for vehicles.

To ensure comfort and safe driving, the environment of the road network and the road pavement should be inspected on a regular basis (Directive 2008/96/EC on audits and inspections). It is one of the principal factors to ensure safety from the road infrastructure perspective.

Dynamics response based road pavement evaluation measures use displacement, or acceleration sensors equipped vehicles or test trailers (Arbabpour Bidgoli et al., 2019; Eshkabilov & Yunusov, 2018; Leitner et al., 2019). This is a convenient and low-cost method, but it evaluates only a specific pavement line – driving track. Specific devices as pavement scanners (Pawar et al., 2018) or image analysis based methods (Inzerillo et al. 2018; Šabanovič et al., 2020) are able to evaluate all pavement surface detecting pavement edge related defects (Qingbo, 2016). Li et al. (2014) identified road cracks using a backpropagation neural network. The rates of correct classification for alligator cracks – 97.5 %, transversal – 100 % and longitudinal cracks – 88.0 %. However, this is more expensive or development and technology application demanding technology. The in-person surveying and observation-based method are

time-consuming and not appropriate for the scope of the current road network (Shtayat et al., 2020). Unfortunately, country roads of lower traffic volume are too seldom maintained, which leads to emerging of pavement defects. The possible solution to deal with road pavement defects is to develop a vehicle chassis system utilising on-vehicle mounted sensors for real-time driving condition estimation or with a driver ability to select a suspension working mode.

2. Tire and suspension part for safe cornering

From a driving perspective, road unevenness directly affects the tire-road interaction, mainly described by adhesion, hysteresis, viscosity and cohesion (Cebon, 1999; Jazar, 2014). However, they do not always appear simultaneously: adhesion is influenced by microstructure, while hysteresis by the macrostructure of the road pavement (Fig. 2a), but
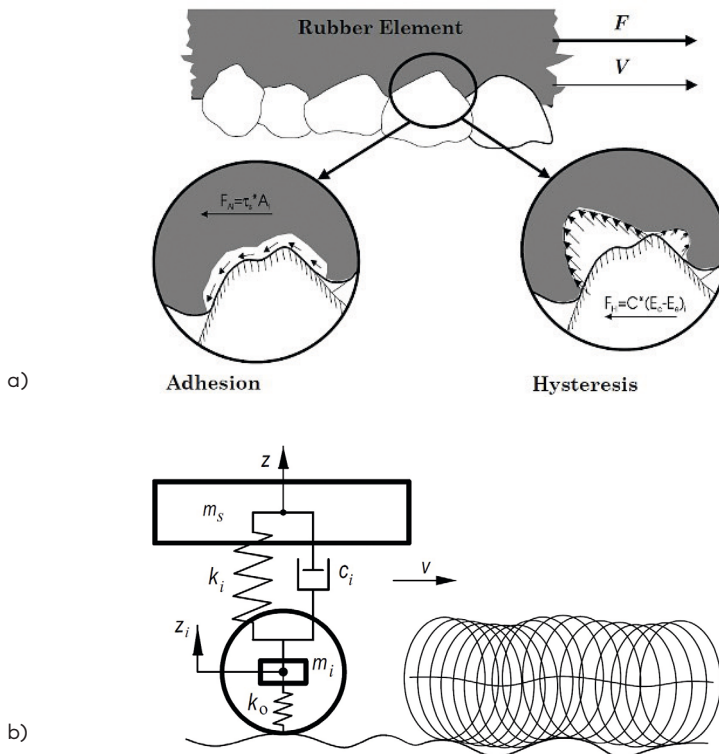

Figure 2. Vehicle – road interaction: a) adhesion and hysteresis between tire and pavement (Hall et al., 2006); b) vertical dynamics of vehicle corner

Vidas Žuraulis,
Vytenis Surblys

Assessment
of Risky Cornering
on a Horizontal Road
Curve by Improving
Vehicle Suspension
Performance

both are related to friction force generation (Chen, 2015). The hysteresis force interacts through the number and form of pavement damage, normal pressure, tangential losses, and it better generates wet grip as well as interaction with the rough road, while adhesion friction acts through intermolecular bounds on smooth – dry pavement.

An important safety factor is the presence of contact of the tire with the road surface while the vehicle is moving on the road pavement of varying smoothness and on road disparities of different shapes (Fig. 2b). Such a movement is mainly affected by stiffness and damping elements of the vehicle tire and suspension (Surblys & Sokolovskij, 2018). Passive damping elements are used in a classic suspension where it is not possible to adapt suspension properties for driving conditions (e.g., pavement roughness level) because damping is only described by hydrodynamics and no supplemental energy for regulation is used (Skrickij et al., 2018). The cost of this type of suspension is lower compared to a semi-active or active suspension. Upon striving to improve the performance of the suspension and ensure the maximum possible driving comfort or to improve the vehicle stability, passive suspensions are replaced with semi-active or active ones (Surblys, 2020). The advanced design with developed control algorithms and supplemental equipment is used to make the regulation or adaptation of suspension performance possible (Žuraulis et al., 2019; Savaresi & Spelta, 2009).

The force in the shock absorber of a semi-active suspension is changed in two ways: by increasing or decreasing the cross-section of the hole in the shock absorber or by changing the viscosity of the liquid. Two acceleration sensors (unsprung and sprung mass mounted) and electronic control unit for data procession in a semi-active suspension are used, but the manual mode selection for the driver is also possible if specific driving conditions are expected or recognised.

3. Vehicle cornering research

Theoretical research by simulating vehicle cornering manoeuvre was conducted to analyse the influence of suspension characteristics on vehicle stabilisation in case of a sharp road curve with deteriorated pavement edge. Fourteen degrees of freedom (DOF) vehicle model was built in MATLAB/Simulink software (Žuraulis & Sokolovskij, 2018). The model covers angular roll, pitch and vertical bounce motion of vehicle body (sprung mass), vertical hop motion of each wheel (unsprung mass), angular rotation of each wheel, and longitudinal, lateral and yaw motion of the whole vehicle. Graphically programmed equations of motion
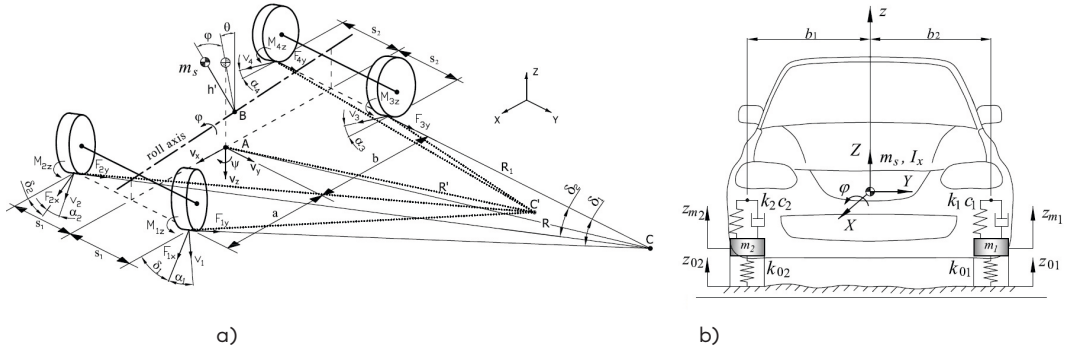
Figure 3. Schemes for vehicle simulation: a) horizontal and roll dynamics
(Žuraulis et al., 2015); b) vertical dynamics

correspond to vehicle dynamics of tire-road interaction, suspension performance, and body motion (Fig. 3). The main parameters for the vehicle simulation model are shown in Table 2.

The input data for MATLAB/Simulink vehicle model were as follows: a steering wheel angle, road pavement elevation for each wheel separately, and throttle torque for drive wheels. Road pavement conditions of dry asphalt were used with maximal friction coefficient μ_{max} = 0.85. The change in the friction coefficient according to tire side-slip, longitudinal slip, as well as other mathematical relations of the used model are presented in the study by Žuraulis and Sokolovskij (2018).

The aim of this research is to analyse the possibility of increasing cornering vehicle stability by changing suspension damping. The semi-active and fully active suspension has an opportunity to control bandwidth at 20 Hz; however, the advantage of semi-active suspension is that it works with very low energy consumption. Semi-active suspension was introduced in 1980 (Savaresi et al., 2010). Many car manufacturers (BMW, GM, Lexus etc.) use this type of shock absorber in their contemporary vehicles (usually as an optional modification). A sensible and correct selection of the suspension damping can reduce the risk to driving safety, e.g., in the circumstances of the deteriorated road surface under consideration.

The nonlinear characteristics of the damping of a semi-active shock absorber are different from the linear ones. To make the theoretical system more similar to the real one, a nonlinear characteristic was chosen. The shock absorber characteristics used in the research are shown in Fig. 4.

Table 2. Parameters for 14 DOF vehicle simulation model

Model parameter	Value	Model parameter	Value
Sprung mass, m_s	1005 kg	Distance from CG to front axle, a	1.12 m
Mass moment of inertia, I_x	526 kg·m²	Distance from CG to rear axle, b	1.49 m
Mass moment of inertia, I_y	1700 kg·m²	Distance from roll axis to CG, h_φ	0.40 m
Mass moment of inertia, I_z	1722 kg·m²	Distance from pitch axis to CG, $h\theta$	0.30 m
Unsprung mass, front, $m_{us1,2}$	40 kg	Tire stiffness, k_{0i}	160 000 N/m
Unsprung mass, rear, $m_{us3,4}$	35 kg	Suspension stiffness, k_i	18 557 N/m
Wheel moment of inertia, $I_{wh.}$	1.9 kg·m²	Suspension damping, c_i	variable
Wheel track, $t_{wh.}$	1.48 m	Vehicle frontal area, $A_{fr.}$	2.1 m
Rolling resistance coef., f_r	0.015	Vehicle air drag coef., c_{air}	0.33

$$F_{cM}(\Delta\dot{z}) = a_0 + a_1 \cdot \cos(d \cdot \Delta\dot{z}) + b_1 \cdot \sin(d \cdot \Delta\dot{z}) + a_2 \cdot \cos(2 \cdot d \cdot \Delta\dot{z}) +$$
$$b_2 \cdot \sin(2 \cdot d \cdot \Delta\dot{z}) + a_3 \cdot \cos(3 \cdot d \cdot \Delta\dot{z}) + b_3 \cdot \sin(3 \cdot d \cdot \Delta\dot{z}) +$$
$$a_4 \cdot \cos(4 \cdot d \cdot \Delta\dot{z}) + b_4 \cdot \sin(4 \cdot d \cdot \Delta\dot{z})$$

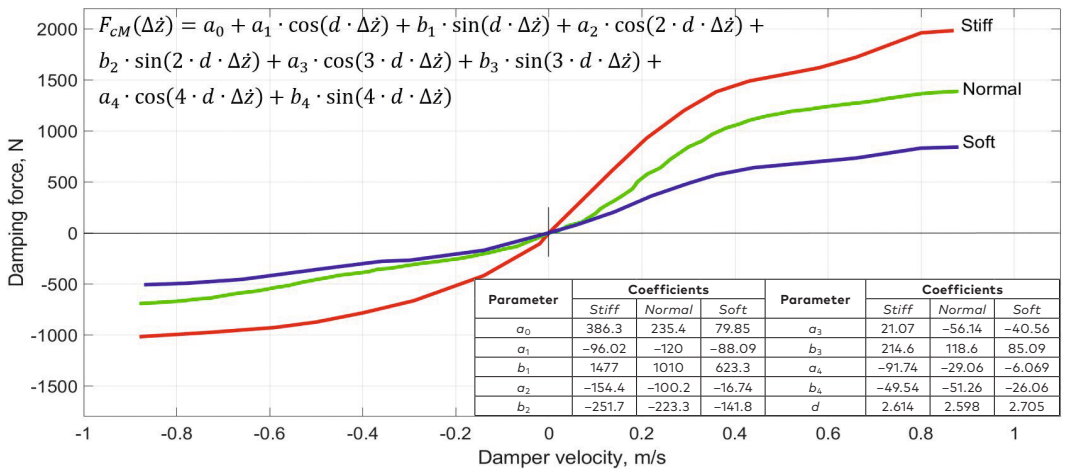| Parameter	Coefficients			Parameter	Coefficients		
	Stiff	Normal	Soft		Stiff	Normal	Soft
a_0	386.3	235.4	79.85	a_3	21.07	−56.14	−40.56
a_1	−96.02	−120	−88.09	b_3	214.6	118.6	85.09
b_1	1477	1010	623.3	a_4	−91.74	−29.06	−6.069
a_2	−154.4	−100.2	−16.74	b_4	−49.54	−51.26	−26.06
b_2	−251.7	−223.3	−141.8	d	2.614	2.598	2.705

Figure 4. Semi-active shock absorber nonlinear damping characteristics with its mathematical description (Ślaski, 2010)

Shock absorber damping force characteristic $F_{cM}(\Delta\dot{z})$ is described by fourth-degree Fourier function (Fig. 4), where $\Delta\dot{z}$ – damper velocity, m/s and $F_{cM}(\Delta\dot{z})$ – damping force, N, (Surblys, 2020).

A higher level of pavement roughness was selected for the input of right side wheels compared to the left one since the right track was considered driving through deteriorated pavement edge during the left turn (Fig. 5). The roughness level of B class according to ISO 8608 standard corresponded to the left vehicle track, while the right one at the

first simulation stage was excited by D class roughness with significantly higher pavement elevation amplitudes and power spectral density (PSD). Such a combination of B and D road class is met in the research of semi-active suspension (Chen et al., 2016a). The standard for pavement roughness and its corresponding road class uses frequency-based description for pavement elevation, while the input of road pavement elevation for vehicle model is expressed in the time domain (Zhang et al., 2007; Chen et al., 2016b):

$$\dot{z}_{0i}(t) = -2\pi v_i n_0 z_{0i}(t) + w(t)\sqrt{G_q(n_0)v_i}\,, \tag{1}$$

where $z_{0i}(t)$ – road elevation input, m, v_i – driving speed, m/s, n_0 – spatial frequency ($n_0 = 0.1$ cycle/m), $w(t)$ – Gaussian white noise with zero mean, $G_q(n_0)$ – road roughness coefficient, which is the value of the road surface PSD under the referred spatial frequency, m^3/cycles, i – the corresponding wheel index.

IRI was calculated for used pavement elevation values (ASTM E1926-08, 2015; Sayers 1995):

$$\mathrm{IRI} = \frac{1}{L}\int_0^{L/v}\left|\dot{z}_s - \dot{z}_{us,i}\right|\mathrm{d}t, \tag{2}$$

where L – length of road profile, m, v – forward vehicle speed applied to a quarter car model, m/s, $_s{}^-$ – velocity of sprung mass vertical displacement, m/s, $_{us,i}|^{\mathrm{d}}$ – velocity of unsprung mass vertical displacement, m/s, dt – time increment, s.

IRI value of 1.21 m/km for the left track and 6.74 m/km for the right track (D class) was determined that indicated good enough road roughness input for inner wheels and high roughness corresponding pavement defects for outer wheels (Fig. 1). These IRI values correspond to the new and damaged pavement, respectively (Sayers & Karamihas, 1998). A similar ratio of roughness levels for smooth sections (0.5 < IRI < 2.0 m/km) and rough sections (2 < IRI < 8 m/km) were found for urban roads in the study by Abulizi et al. (2016); also the decrease of IRI from 1.74 m/km to 5.74 m/km was indicated after six years of road exploitation (Vázquez et al., 2020). Moreover, Múčka (2019) measured roughness distribution for lateral road profile and evaluated that IRI values were 3 times higher at the right edge line for second class roads. These results confirm the correct choice of road roughness class for the cornering stability simulation presented in this paper, assuming that cracks for pavement edge are involved. Selected ISO 8608 road classes B and D also correctly correspond to a very good and mediocre ride quality with IRI values of 1.43–2.84 m/km and >4.05 m/km, respectively, defined by Loprencipe et al. (2019). However, a higher road roughness of
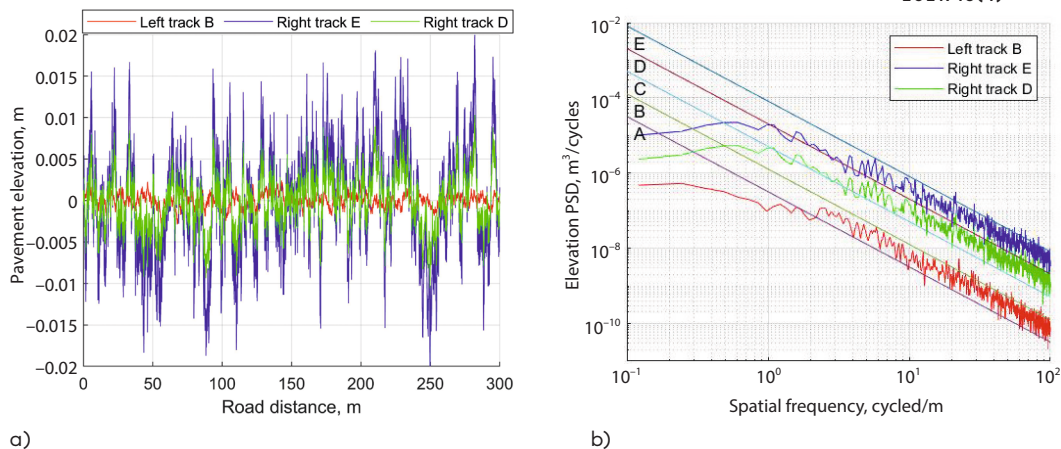
Figure 5. Road pavement input for vehicle model: a) pavement elevation as per road distance; b) elevation spectral density representation according to ISO 8608 classification

class E (Fig. 5) was also involved in this research later as the cracks of pavement edge eventually deteriorated significantly (Fig. 1).

The cornering on the horizontal road curve was initiated from the 15th simulation second, then the vehicle speed stabilised. The vehicle front wheels were steered by an average value of 1.28 degrees, maintaining the provided vehicle trajectory of 120 m radius. Such a radius was selected because the range of radius between 150 and 200 meters was the most frequent for regional roads in curved sections (Bíl et al., 2018). Pavement superelevation of 4% according to national regulation was used in the simulation (Kelių techninis reglamentas, 2008). The throttle for drive wheels was kept constant for the whole trajectory of the cornering manoeuvre; however, vehicle velocity slightly decreased because of additional side-slip resistance. The cases of 80, 90, and 100 km/h driving were selected for this analysis, as they were close enough to the vehicle stability limit at these conditions. The obtained lateral acceleration between 6–8 m/s^2 and body side-slip angle between 5–14 degrees confirm high cornering intensity.

As it was mentioned in Section III, suspension by its damping force ensures the maximal possible tire contact duration with the pavement. The damping force of suspension is produced in relation to its deflection velocity; therefore, the characteristic of deflection velocity during the simulated cornering manoeuvre is shown in Fig. 6. As simulation was performed using three suspension damping characteristics (Fig. 4), the results for better difference identification were shown by *Soft* and *Stiff*
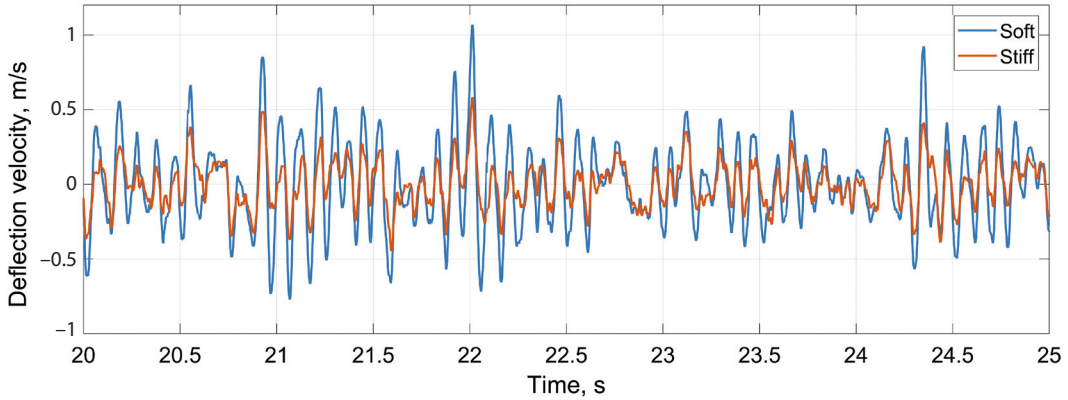
Figure 6. Suspension deflection velocity of the most loaded front right vehicle corner at different damping modes (D class, 90 km/h)

modes only and for 90 km/h as the best representative here. It is seen from Fig. 6 that for the same driving conditions (speed, trajectory and road input), the suspension movement in *Soft* mode is significantly faster compared to *Stiff* mode.

To realise better the suspension deflection differences working in *Soft/Normal/Stiff* modes, the Root Mean Square (RMS) values were calculated:

$$\text{RMS}_{\dot{z}_i} = \left[\frac{1}{T} \int_0^T \Delta \dot{z}_{susp.}^2 \, dt \right]^{1/2}, \tag{3}$$

where $\dot{z}_{susp.}$ – velocity of suspension deflection, m/s, T – duration of the manoeuvre, s, dt – time increment, s.

Although deflection velocity of suspension is related to damping of unsprung mass fluctuations, it is also influenced by sprung mass dynamics and therefore does not represent vehicle stability unambiguously. Therefore, the Dynamic Load Coefficient (DLC) was used to evaluate tire contact with the pavement. DLC is calculated as the ratio between the variation of vertical tire force with the static tire force F_{stat} (Cebon, 1999; Mitschke & Wallentowitz, 2014):

$$\text{DLC} = \frac{\text{RMS}_{Fz,\text{dyn}}}{F_{\text{stat}}}, \tag{4}$$

where $\text{RMS}_{Fz,dyn}$ – root mean square of dynamic vertical tire force ($F_{z,\text{dyn}}$) determined from vehicle model simulation or by:

$$F_{z,\text{dyn}} = k_{0i} \left(z_{us} - z_o \right), \tag{5}$$

Vidas Žuraulis,
Vytenis Surblys

Assessment
of Risky Cornering
on a Horizontal Road
Curve by Improving
Vehicle Suspension
Performance

where k_{0i} – tire radial stiffness, z_{us} – unsprung mass (wheel with corresponding axle mass) vertical displacement, z_o – vertical elevation of road pavement.

The results of suspension deflection velocity and DLC of 90 km/h driving speed are shown in Table 3. A significant difference between the left and right track for both suspension velocity and DLC is explained by a different level of roughness used (B and E class). The influence of suspension damping mode reveals the achieved potential of vehicle stability. The lowest fluctuations of suspension velocity are achieved using *Stiff* damping mode that influences tire–pavement interaction recognised as DLC. The DLC has a slight variation for the left side wheel because of the low pavement roughness level; however, the important differences are for the right one. Here *Stiff* damping mode causes the lowest DLC values corresponding to smooth enough tire contact duration with the pavement and better vehicle stability. Generally, the range of DLC is between 0.01 and 0.4, with better tire contact, i.e., lower values. The value of DLC = 0.3 is considered a safety threshold when the loss of contact between tire and road can occur for about 0.135% of duration (Múčka, 2016). In addition, DLC value tends to increase with the increasing vehicle speed at the same road conditions (Cebon, 1999). As it is seen, the DLC is closer to the safety threshold with the *Soft* damping mode at the right side wheels.

Extended results of DLC for different road classes, driving speeds, and selected suspension damping modes are shown in Fig. 7. Only the right track interacting with two different road class roughness values is selected here as DLC for the left track is much lower (seen from Table 3) because it mostly keeps on smooth enough central part of the road. The interaction with lower roughness class pavement naturally reveals better road holding with lower than 0.3 DLC for all simulation cases.

Table 3. Generalised results of suspension deflection velocity and dynamic load coefficient (DLC)

Suspension damping mode	RMS of suspension deflection velocity, m/s				DLC			
	Left track (B class)		Right track (D class)		Left track (B class)		Right track (D class)	
	Front	Rear	Front	Rear	Front	Rear	Front	Rear
Soft	0.057	0.057	0.285	0.285	0.042	0.062	0.203	0.252
Normal	0.048	0.048	0.218	0.218	0.041	0.061	0.180	0.225
Stiff	0.041	0.041	0.162	0.160	0.042	0.067	0.173	0.216

However, *Stiff* damping mode and *Normal* one demonstrate better results compared to *Soft* mode.

Higher roughness for the right track induces a slightly increasing difference between damping modes, but the *Soft* one still keeps the highest DLC values (worse road holding). Moreover, vehicle cornering over highly deteriorated outer track pavement approaches the safety threshold. DLC exceeds 0.3 value for the rear axle at 80 and 90 km/h and for both axles at 100 km/h. It was also recognised from the obtained DLC values that *Normal* damping mode was closer to *Stiff* one, i.e., better selection than *Soft* damping seeking for good enough vehicle control and stability.

The right-side wheels are more loaded by roll moment transmitted from the vehicle centre of gravity (CG) when CG receives the centrifugal force of the cornering vehicle. A higher normal force on a wheel theoretically increases friction force; however, under the analysed case, the fluctuations caused by deteriorated road pavement decrease tire contact forces. The obtained results meet the research of flexible pavement and truck interaction, where a lower variation of wheel and body displacement, as well as dynamic pavement load had higher suspension damping (Elnashar et al., 2019). Moreover, comparable research showed that spectral density of normal tire force had a lower magnitude for unsprung mass natural frequency (11–15 Hz), while the increase in the speed or roughness increased tire force already from 3 Hz of excitation (Yang et al., 2015). The obtained trends are also confirmed by theoretical and experimental research utilising semi-active suspension, where the decrease in road disturbance under
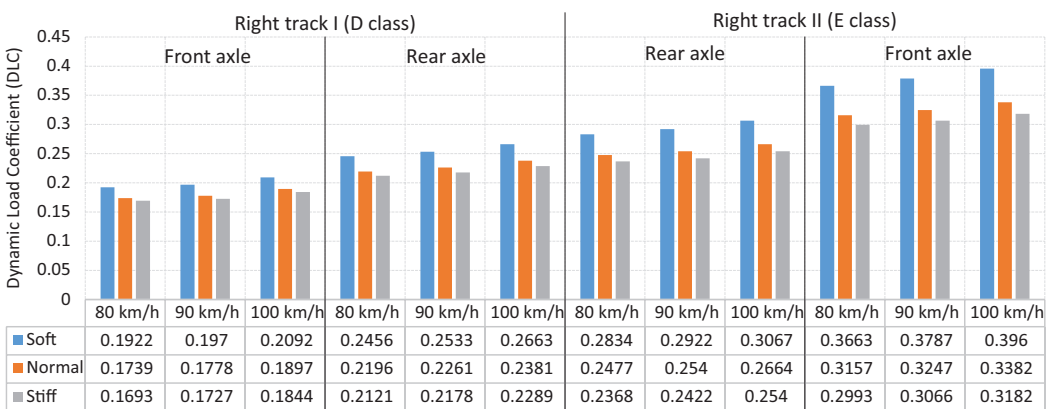
	Right track I (D class)						Right track II (E class)					
	Front axle			Rear axle			Rear axle			Front axle		
	80 km/h	90 km/h	100 km/h	80 km/h	90 km/h	100 km/h	80 km/h	90 km/h	100 km/h	80 km/h	90 km/h	100 km/h
Soft	0.1922	0.197	0.2092	0.2456	0.2533	0.2663	0.2834	0.2922	0.3067	0.3663	0.3787	0.396
Normal	0.1739	0.1778	0.1897	0.2196	0.2261	0.2381	0.2477	0.254	0.2664	0.3157	0.3247	0.3382
Stiff	0.1693	0.1727	0.1844	0.2121	0.2178	0.2289	0.2368	0.2422	0.254	0.2993	0.3066	0.3182

Figure 7. DLC for different road classes, driving speeds and suspension damping modes

Vidas Žuraulis,
Vytenis Surblys

Assessment
of Risky Cornering
on a Horizontal Road
Curve by Improving
Vehicle Suspension
Performance

A–E road roughness classes with increasing suspension damping was obtained (Liu et al., 2020). Higher damping in semi-active suspension also improves the combined ride comfort – suspension spacing – road holding indicator (Chen et al., 2016a).

The lateral distance differences of vehicle trajectory driving under specific suspension damping mode were calculated according to the equation:

$$\Delta S_{lat.} = \cos\left(90 - \psi_{ref.} + \Delta\psi\right) \cdot \Delta S, \tag{6}$$

where: $\psi_{ref.}$ – vehicle yaw angle with reference damping mode (*Stiff*), $\Delta\psi$ – yaw angle difference between a vehicle with reference (*Stiff*) and relevant (*Normal* or *Soft*) damping mode, ΔS – the distance between a vehicle with reference (*Stiff*) and relevant (*Normal* or *Soft*) damping mode.

Yaw angle difference and distance between a vehicle with reference and relevant damping mode were calculated by:

$$\Delta\psi = \cos^{-1}\left(\frac{X_{ref.}X_{rel.} + Y_{ref.}Y_{rel.}}{\sqrt{X_{ref.}^2 + Y_{ref.}^2} \cdot \sqrt{X_{rel.}^2 + Y_{rel.}^2}}\right), \tag{7}$$

$$\Delta S = \sqrt{\left(X_{ref.} - X_{rel.}\right)^2 + \left(Y_{ref.} - Y_{rel.}\right)^2}, \tag{8}$$

where: $X_{ref.}$ and $Y_{ref.}$ – abscissa and ordinate of the instantaneous position of the vehicle with reference damping mode, $X_{rel.}$ and $Y_{rel.}$ – abscissa and ordinate of the instantaneous position of the vehicle with relevant damping mode.

The calculated difference of vehicle trajectory driving under specific suspension damping mode (Eq. 7) for different speeds is shown in Fig. 8. *Stiff* damping mode was selected as a reference. Maintaining of vehicle cornering stability is most significant during the first corner part (before the apex); therefore, the distribution of trajectory differences at different speeds will be analysed between the 14th and 18th second of simulation. The trajectory using *Normal* damping mode does not differ much (around 0.05 m) from the reference trajectory (*Stiff* damping mode). A slight increase was recognised at higher speeds up to the corner apex. However, a more significant difference (for around 0.3 m) was obtained between trajectory using *Soft* damping mode and reference trajectory. The same increase of trajectory difference was recognised at higher speeds in the first corner part as previously.

For better evaluation of the advantage of specific suspension damping selection, the increase in road roughness for right-side pavement edge per unevenness class (up to class E) was involved in
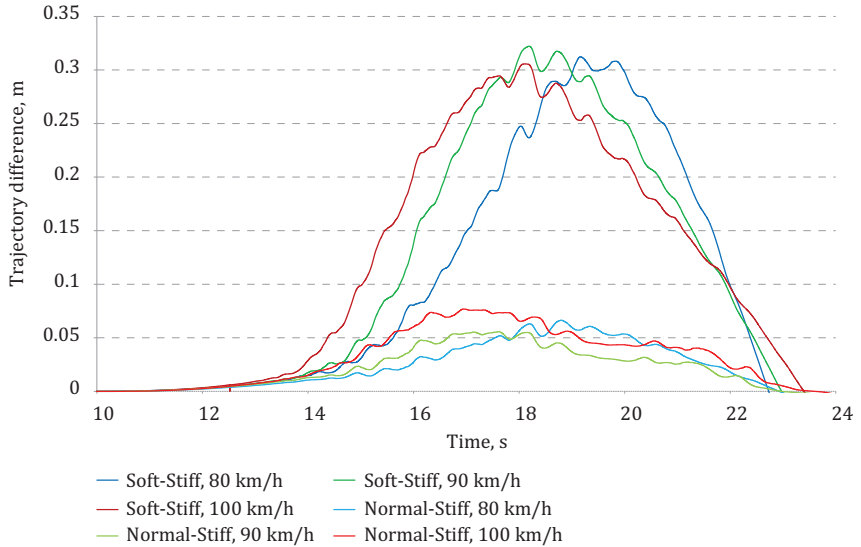
Figure 8. Trajectory differences with different suspension damping modes and driving speeds on D class road for the right track

vehicle cornering simulations. The graph of trajectory differences in this case for different speeds is shown in Fig. 9. The same tendency as for a case of D class road but with a small increase in trajectory differences (up to 0.1 m) was obtained between *Normal* damping mode and reference trajectory (*Stiff* damping mode). The difference between *Soft* damping mode and reference trajectory after reaching rough enough pavement edge remained dangerous even with an increase up to 0.45 m. Such lateral vehicle shifting is critical and corresponds to a full loss of vehicle control with possible reach of an unpaved road shoulder or slipping off the road.

For interaction with both D and E class roads, the cases of 100 km/h speed have an earlier stage of higher slip (dark red colour curves in Figs. 8 and 9). It means that for the same speed and steering control, the vehicle already starts slipping even before it reaches the maximum steering angle at the 15th cornering second. The dark red colour curve of the trajectory difference separates from others at the 14th second. Earlier initial slipping gives some more time for the driver to stabilise the vehicle, reduce its speed or at least realise the situation. Vehicle understeering accrues in this situation from a bit higher front axle side-slip angle compared to the lack of rear axle, and this is more conducive for an ordinary-skilled nonprofessional driver. At a lower speed (dark blue colour curve), the slip is slightly delayed, as the vehicle does not
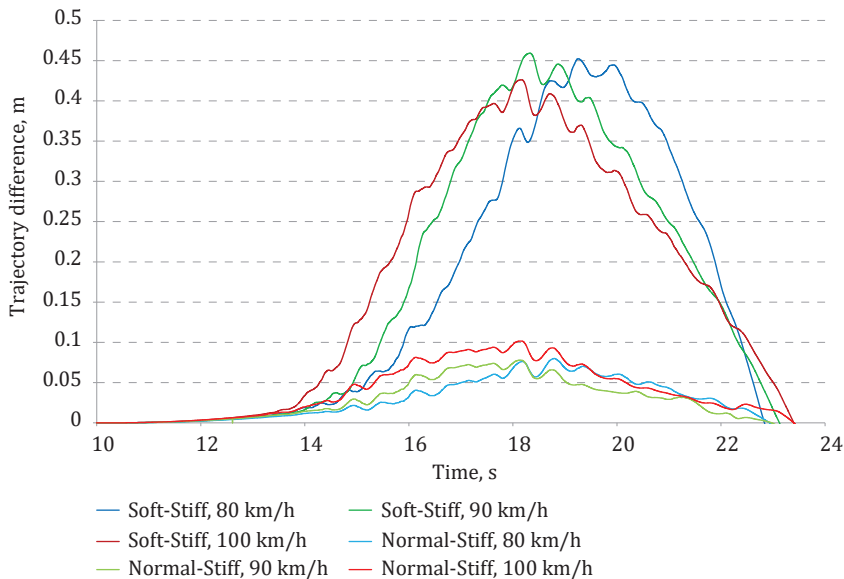
Vidas Žuraulis,
Vytenis Surblys

Assessment
of Risky Cornering
on a Horizontal Road
Curve by Improving
Vehicle Suspension
Performance

Figure 9. Trajectory differences with different suspension damping modes and driving speeds on E class road for the right track

reach the stability limit at the beginning of the corner; however, at the corner apex (19–20th second), the trajectory difference reaches the same critical values as at 90 and 100 km/h. The analysis shows that the *Soft* damping mode does not provide sufficient stability reserve for the vehicle moving in critical cornering conditions, while the *Normal* and *Stiff* damping modes may give the driver more options to keep the vehicle in control and stability. These tendencies were analysed and evaluated for one specific corner case but at different driving speeds and different roughness levels of the road edge. However, the observed trends in wheel interaction with high road roughness and different suspension damping modes are applicable to other driving cases (e.g., intense braking) where suspension operation has a significant effect on normal wheel load and generated grip forces directly affecting vehicle control and road safety.

Soft damping mode can provide a sufficiently good level of driving comfort (Yang et al., 2021), but is not suitable to maintain good enough handling for driving on poor quality road surfaces when the insufficient road holding is caused by excessive tire grip force fluctuation (Guiggiani, 2014).

Vehicle unsprung mass fails to adapt to existing road roughness at an excessive speed or aggressive manoeuvre due to limited suspension

damping. However, *Normal* or *Stiff* modes of suspension damping change the characteristics of the shock absorber; therefore, it generates higher damping forces at the same suspension deflection velocity resulting in better driving stability. The significant correction of the cornering trajectory of 0.3–0.35 m is achievable by selecting the appropriate suspension damping mode. Nevertheless, timely and periodic implementation of road maintenance and its safety management even at rural regional roads will lead to effective accident prevention, while the development of vehicle suspension performance at different pavement states is ready to compensate for driver's error or inattention.

Conclusions

Road pavement plays a particularly important role in ensuring vehicle stability, and it is a broad research area being analysed in the context of pavement type and state, geometrical parameters or used safety measures worldwide. Accidents on horizontal road curves are specifically influenced by limited sight distance and driver's fault to predict curve geometry or safe driving speed. Moreover, the accidents are caused due to the lack of rural two-line regional (secondary) road renewal and maintenance from a road safety point of view. Deteriorated edge of road pavement with cracks is a characteristic feature in regions with a changing climate. Moreover, the impact of wheel loads, especially from the trucks, increases pavement damage significantly. Insufficient priority for safety management of these roads leads to an increase in the potential accident rate.

The situation when the design speed of the rural regional road is lower than the permissible speed at a specific sharp horizontal curve was analysed in this research from a vehicle stability point of view. The possible shift of vehicle cornering trajectory can be induced by the cracks of the road pavement, and it leads to a possible accident on a sharp horizontal road curve. The possibility to increase vehicle stability by regulated suspension damping force characteristic was simulated using 14 degrees of freedom vehicle dynamic model in MATLAB/Simulink software. The influence of deteriorated edge of road pavement was modelled by higher roughness input for outer vehicle wheel in relation to the turning trajectory. Suspension with higher damping force characteristic (*Stiff* damping) showed better vehicle stability results, despite the fact that the performance of vehicle dynamics was strongly nonlinear and depended on a combination of suspension

Vidas Žuraulis,
Vytenis Surblys

Assessment
of Risky Cornering
on a Horizontal Road
Curve by Improving
Vehicle Suspension
Performance

stiffness-damping as well as tire-road interaction. The deviation from the driving trajectories utilising different suspension damping modes was from 0.05 to 0.3 m when wheels of the outer cornering side interacted with road pavement of D class roughness. A larger trajectory difference occurred when shock absorbers were adjusted to *Soft* damping mode on the rough pavement (road class D) when suspension did not inhibit pavement excited vibrations. Similar tendencies were obtained for 80–100 km/h driving speeds used in simulations; however, an increase in trajectory difference up to dangerous 0.45 m was found after extending the simulations on more rough E class road pavement, when wheels reached the pavement edge or roadside.

Better tire-road interaction working on *Stiff* damping mode was also comfirmed by Dynamic Load Coefficient. Estimated DLC values were lower (better road holding) for all cases of analysed speeds (80–100 km/h) and pavement roughness (D and E class); however, too high DLC was found when outer wheels of cornering vehicle interacted with higher roughness (E class) road pavement. At this case, the safety threshold for road holding was exceeded with all three suspension damping modes for rear vehicle axle and with *Soft* damping mode for front axle.

In such a case, fast and precise action by the driver is required; however, some delays of reaction or inaccuracy of actions is possible to compensate by suspension damping control. Road adjusted suspension decreases wheel contact loss, vehicle outward displacement, and risk of a possible accident. The benefits of changing the damping force of suspension for specific driving modes or conditions meet the research of other scientists (Savaresi et al., 2010; Liu et al., 2013; Suzuki & Takahashi, 2012).

The presented research results of vehicle driving simulation at a specific road section with several vehicle stability influencing factors (such as road curves, roughness, friction levels, etc.) in the future could be used for risk evaluation and prediction of possible road accidents. Computer simulation is an accurate, timely and cost-effective tool to evaluate various scenarios of vehicle and road interaction.

Acknowledgment

REFERENCES

AASHTO. (2008). *American Association of State Highway and Transportation Officials. Driving Down Lane-Departure Crashes: A National Priority.*

AASHTO. (2010). *Highway Safety Manual. American Association of State Highway Transportation Officials, Washington, D.C.*

Abulizi, N., Kawamura, A., Tomiyama, K., Fujita, Sh. (2016). Measuring and evaluating of road roughness conditions with a compact road profiler and ArcGIS. *Journal of Traffic and Transportation Engineering (English Edition)*, *3*(5), 398–411. https://doi.org/10.1016/j.jtte.2016.09.004

Ahmad, T., & Khawaja, H. (2018). Review of Low-Temperature Crack (LTC) Developments in Asphalt Pavements. *The International Journal of Multiphysics*, *12*(2), 169–187. https://doi.org/10.21152/1750-9548.12.2.169

Aram, A. (2010). Effective Safety Factors on Horizontal Curves of Two-lane Highways. *Journal of Applied Sciences*, *10*(22), 2814–2822. https://doi.org/10.3923/jas.2010.2814.2822

Arbabpour Bidgoli, M., Galroo, A., Sheikhzadeh Nadjar, H., Rashidabad A. G., & Reza Ganji, M. (2019). Road Roughness measurement using a cost effective sensor-based monitoring system. *Automation in Construction*, *104*, 140–152. https://doi.org/10.1016/j.autcon.2019.04.007

ASTM E1926-08. (2015). *Standard practice for computing International Roughness Index of Roads from longitudinal profile measurements.* ASTM International.

Bíl, M., Andrášik, R., & Sedoník, J. (2019). Which curves are dangerous? A network-wide analysis of traffic crash and infrastructure data. *Transportation Research Part A: Policy and Practice*, *120*, 252–260. https://doi.org/10.1016/j.tra.2019.01.001

Bíl, M., Andrášik, R., Sedoník, J., & Cícha, V. (2018). ROCA – An ArcGIS toolbox for road alignment identification and horizontal curve radii computation. *PLoS ONE 13*(12). https://doi.org/10.1371/journal.pone.0208407

Bogenreif, C., Souleyrette, R. R., & Hans, Z. (2012). Identifying and Measuring Horizontal Curves and Related Effects on Highway Safety. *Journal of Transportation Safety & Security*, *4*(3), 179–192. https://doi.org/10.1080/19439962.2011.646001

Calvi, A. (2015). A Study on Driving Performance Along Horizontal Curves of Rural Roads. *Journal of Transportation Safety & Security*, *7*(3), 243–267. https://doi.org/10.1080/19439962.2014.952468

Canestrari, F., & Ingrassia, L. P. (2020). A review of top-down cracking in asphalt pavements: Causes, models, experimental tools and future challenges. *Journal of Traffic and Transportation Engineering*, *7*(5), 541–572. https://doi.org/10.1016/j.jtte.2020.08.002

Cebon, D. (1999). *Handbook of vehicle-road interaction*. CRC Press.

Chen, M. Z. Q., Hu, Y., Li, C., & Chen, G. (2016a). Application of Semi-Active Inerter in Semi-Active Suspensions Via Force Tracking. *Journal of Vibration and Acoustics*, *138*(4), 041014. https://doi.org/10.1115/1.4033357

Vidas Žuraulis,
Vytenis Surblys

Assessment
of Risky Cornering
on a Horizontal Road
Curve by Improving
Vehicle Suspension
Performance

Chen, W., Xiao, H., Wang, Q., Zhao, L., & Zhu, M. (2016b). *Integrated Vehicle Dynamics and Control*. John Wiley & Sons. https://doi.org/10.1002/9781118380000

Chen, X. (2015). From Texture to Skid Resistance: A Multi-Scale Modelling Approach. *Journal of Testing and Evaluation*, *2*, 465–471. https://doi.org/10.1520/JTE20130291

Cheng, G., Cheng, R., Pei, Y., & Xu, L. (2020). Probability of Roadside Accidents for Curved Sections on Highways. *Mathematical Problems in Engineering*, *2020*, Article ID 9656434. https://doi.org/10.1155/2020/9656434

Dirección General de Tráfico (DGT). (2015). http://www.dgt.es/es/seguridad-vial/estadisticas-e-indicadores/

Directive 2008/96/EC of the European Parliament and of the Council of 19 November 2008 on road infrastructure safety management.

Eboli, L., Forciniti, C., & Mazzulla, G. (2020). Factors influencing accident severity: an analysis by road accident type. *Transportation Research Procedia*, *47*, 449–456. https://doi.org/10.1016/j.trpro.2020.03.120

Elvik, R. (2013). International transferability of accident modification functions for horizontal curves. *Accident Analysis and Prevention*, *59*, 487–496. http://dx.doi.org/10.1016/j.aap.2013.07.010

Elvik, R. (2019). The more (sharp) curves, the lower the risk. *Accident Analysis and Prevention*, *113*, 105322. https://doi.org/10.1016/j.aap.2019.105322

Elnashar, G., Bhat, R. B., & Sedaghati, R. (2019). Modeling and dynamic analysis of a vehicle-flexible pavement coupled system subjected to road surface excitation. *Journal of Mechanical Science and Technology*, *33*(7), 3115–3125. https://doi.org/10.1007/s12206-019-0606-5

ERA-NET ROAD. (2012). *Safety at the Heart of Road Design. Final Report of the ERA-NET programme.*

Eshkabilov, S., & Yunusov, A. (2018). Measuring and Assessing Road Profile by Employing Accelerometers and IRI Assessment Tools. *American Journal of Traffic and Transportation Engineering*, *3*(2), 24–10. https://doi.org/10.11648/j.ajtte.20180302.12

European Commission. (2010*). Towards a European road safety area: policy orientations on road safety 2011–2020* (COM(2010) 389 final of 20 July 2010).

European Commission. (2018). *Road Safety 2018. How is your country doing?* https://ec.europa.eu/transport/road_safety/sites/roadsafety/files/pdf/scoreboard_2018_en.pdf

Federal Highway Administration, U.S. Department of Transportation. (2014). *Safety Effects of Horizontal Curve and Grade Combinations on Rural Two-Lane Highways*. Report, FHWA-HRT-13-078.

Furlan, A. D., Kajaks, T., Tiong, M., Lavallière, M., Campos, J. L., Babineau, J., Haghzare, S., Ma, T., & Vrkljan, B. (2020). Advanced vehicle technologies and road safety: A scoping review of the evidence. *Accident Analysis & Prevention, 147*, 105741. https://doi.org/10.1016/j.aap.2020.105741.

Gooch, J. P., Gayah, V. V., & Donnell. E. T. (2016). Quantifying the safety effects of horizontal curves on two-way, two-lane rural roads. *Accident Analysis and Prevention, 92*, 71–81. http://dx.doi.org/10.1016/j.aap.2016.03.024

Guiggiani, M. (2014). *The Science of Vehicle Dynamics. Handling, Braking, and Ride of Road and Race Cars*. Springer.

Hall, J. W., Smith, K. L, Titus-Glover, L., Wambold, J. C., Yager, T. J., & Rado, Z. (2006). *Guide for Pavement Friction. NCHRP Project* 1-43, *National Cooperative Highway Research Program (NCHRP), Washington, D.C.*

Høye, A. (2020). Speeding and impaired driving in fatal crashes—Results from in-depth investigations. *Traffic Injury Prevention, 21*(7), 425–430. https://doi.org/10.1080/15389588.2020.1775822

Hummer, J. E., Rasdorf, W., Findley, D. J., Zegeer, Ch. V., & Sundstrom, C. A. (2010). Curve Collisions: Road and Collision Characteristics and Countermeasures. *Journal of Transportation Safety & Security*, *2*(3), 203–220. https://doi.org/10.1080/19439961003734880

Inzerillo, L., Di Mino, G., & Roberts, R. (2018). Image-based 3D reconstruction using traditional and UAV datasets for analysis of road pavement distress. *Automation in Construction*, *96*, 457–469. https://doi.org/10.1016/j.autcon.2018.10.010

ISO 8608:1995. *Mechanical vibration – Road surface profiles – Reporting of measured data.*

Jazar, R. N. (2014). *Vehicle Dynamics: Theory and Application*. Springer.

Kelių techninis reglamentas, (2008). KTR 1.01:2008 *Automobilių keliai* [Road technical regulation. Roads for land vehicles].

Lamm, R., Psarianos, B., & Mailaender, T. (1999). *Highway Design and Traffic Safety Engineering: Handbook*. McGraw Hill.

Leitner, B., Decký, M., & Kováč, M. (2019). Road pavement longitudinal evenness quantification as stationary stochastic process. *Transport*, *34*(2), 195–203. https://doi.org/10.3846/transport.2019.8577

Leonovič, I., Laurinavičius, A., & Čygas, D. (2013). *Keliai ir klimatas*. Technika.

Li, L., Sun, L., Ning, G., & Tan, S. (2014). Automatic pavement crack recognition based on BP neural network. *Promet – Traffic & Transportation*, *26*(1), 11-22. https://doi.org/10.7307/ptt.v26i1.1477

Lithuanian Road Police. (2020). *Annual road accident report*.

Liu, H., Gao, H., Li, P. (2013). *Handbook of vehicle suspension control systems.* The Institution of Engineering and Technology.

Liu, W., Wang, R., Ding, R., Meng, X., & Yang, L. (2020). On-line estimation of road profile in semi-active suspension based on unsprung mass acceleration. *Mechanical Systems and Signal Processing*, *135*, 106370. https://doi.org/10.1016/j.ymssp.2019.106370

Loprencipe, G., Zoccali, P., & Cantisani, G. (2019). Effects of Vehicular Speed on the Assessment of Pavement Road Roughness. *Applied Sciences*, *9*, 1783. https://doi.org/10.3390/app9091783

Maljković, D., & Cvitanić, D. (2016). Evaluation of design consistency on horizontal curves for two-lane state roads in terms of vehicle path radius and speed. *The Baltic Journal of Road and Bridge Engineering*, *11*(2), 127–135. https://doi.org/10.3846/bjrbe.2016.15

Mastinu, G., & Ploechl, M. (2014). Road and Off-Road Vehicle System Dynamics Handbook. CRC Press.

Vidas Žuraulis,
Vytenis Surblys

Assessment
of Risky Cornering
on a Horizontal Road
Curve by Improving
Vehicle Suspension
Performance

Mitschke, M., Wallentowitz, H. (2014). *Dynamik der Kraftfahrzeuge*. Springer.

Miller, J. S., & Bellinger, W. Y. (2014). Distress identification manual for the long-term pavement performance program (No. FHWA-RD-13-092). United States. Federal Highway Administration. Office of Infrastructure Research and Development.

Múčka, P. (2016). Road Roughness Limit Values Based on Measured Vehicle Vibration. *Journal of Infrastructure Systems*, *23*(2), 1–13. https://doi.org/10.1061/(ASCE)IS.1943-555X.0000325

Múčka, P. (2019). Influence of profile specification on International Roughness Index. *Journal of Infrastructure Systems*, *25*(2), 1–14. https://doi.org/10.1061/(ASCE)IS.1943-555X.0000478

Othman, S., Thomson, R., & Lannér, G. (2010). Are Driving and Overtaking on Right Curves More Dangerous than on Left Curves? *Ann Adv Automot Med.*, *54*, 253–264.

Paukštė, J. (2015). *Strateginio planavimo ir vystymo modelio analizė, vertinimas ir taikymas* Šiaulių *regiono magistralinių kelių tinklo valdymui*. Vilnius.

Pawar, P. R., Mathew, A. T. & Saraf, M. R. (2018). IRI (International Roughness Index): An Indicator of Vehicle Response. *Materials Today: Proceedings*, *5*(5), 11738–11750. https://doi.org/10.1016/j.matpr.2018.02.143

PIARC Technical Committee on Road Safety. (2003). *Road Safety Manual.* World Road Association.

Qingbo, Z. (2016). Pavement crack detection algorithm based on image processing analysis. *2016 8th International Conference on Intelligent Human-Machine Systems and Cybernetics*, 15–18. https://doi.org/10.1109/IHMSC.2016.96

Queensland Transport. (2006). *Webcrash 2.3: Queensland Government*.

Rakotonirainy, A., Chen, S., Scott-Parker, B., Loke, S. W., & Krishnaswamy S. (2015). A Novel Approach to Assessing Road-Curve Crash Severity. *Journal of Transportation Safety & Security*, *7*(4), 358–375. https://doi.org/10.1080/19439962.2014.959585

Šabanovič, E., Žuraulis, V., Prentkovskis, O., & Skrickij, V. (2020). Identification of Road-Surface Type Using Deep Neural Networks for Friction Coefficient Estimation. *Sensors*, *20*(3), 0612. https://doi.org/10.3390/s20030612

SafetyNet. (2010). *Accident causation database 2005 to 2008.* European Commision.

Savaresi, S. M., & Spelta, C. (2009). A single-sensor control strategy for semi-active suspensions. *IEEE Transactions on Control Systems Technology*, *17*(1), 143–152. https://doi.org/10.1109/TCST.2008.906313

Savaresi, S. M., Poussot-Vassal, C., Spelta, C., Sename, O., & Dugard, L. (2010). *Semi-Active Suspension Control Design for Vehicles*. Butterworth-Heinemann/ Elsevier.

Sayers, M. W. (1995). On the calculation of international roughness index from longitudinal road profile. *Transportation Research Record, 1501*, 1–12.

Sayers, M. W. & Karamihas, S. M. (1998). *The little book of profiling*. University of Michigan, MI.

Schiehlen, W., & Iroz, I. (2015). Uncertainties in Road Vehicle Suspensions. *Procedia IUTAM*, *13*, 151–159. https://doi.org/10.1016/j.piutam.2015.01.016

Šeporaitis, M., Vorobjovas, V., & Vaitkus, A. (2020). Evaluation of Horizontal Curve Radius Effect on Driving Speed in Two Lane Rural Road. Pilot Study. *The Baltic Journal of Road and Bridge Engineering*, *15*(4), 252–270. https://doi.org/10.7250/bjrbe.2020-15.503

Shields, B., Morris, A., Jo, B., & Fildes, B. (2001). *Australia's National Crash In-depth Study Progress Report.* Monash University, Accident Research Centre.

Shtayat, A., Moridpour, S., Best, B., Shroff, A., & Raol, D. (2020). A review of monitoring systems of pavement condition in paved and unpaved roads. J. *Traffic Transp. Eng. 7*(5), 629–638. https://doi.org/10.1016/j.jtte.2020.03.004

Shuler, S., & Nobe, M. D. (2007) Edge Cracking in residential development hot mix asphalt pavements. *International Journal of Construction Education and Research*, *3*, 179–197. https://doi.org/10.1080/15578770701715029

Sivilevičius, H., & Vansauskas, V. (2013). Research and evaluation of ruts in the asphalt pavement on Lithuanian highways. *Journal of Civil Engineering and Management*, *19*(5), 609–621. https://doi.org/10.3846/13923730.2013.817481

Sivilevičius, H., Bražiūnas, J., & Prentkovskis, O. (2017). Technologies and principles of hot recycling and investigation of preheated reclaimed asphalt pavement batching process in an asphalt mixing plant. *Applied sciences, 7*(11), 1–20. https://doi.org/10.3390/app7111104

Skrickij, V., Savitski, D., Ivanov, V., & Skačkauskas, P. (2018). Investigation of cavitation process in monotube shock absorber. *International Journal of Automotive Technology*, *19*(5), 801–810. https://doi.org/10.1007/s12239-018-0077-1

Ślaski, G. (2010). Damping parameters of suspension of a passenger vehicle equipped with semi-active dampers with a by-pass valve. *Transport Problems*, *6*(5), 35–42.

Surblys, V. (2020). *Nelygia kelio danga važiuojančio lengvojo automobilio pusiau aktyvios pakabos valdymo algoritmai*. Technika. https://doi.org/10.20334/2020-003-M

Surblys, V., & Sokolovskij, E. (2018). The research of passenger car passive and semi-active suspension. *Mokslas – Lietuvos ateitis / Science – Future of Lithuania*, *10*, 1–5. https://doi.org/10.3846/mla.2018.6050

Suzuki, T., & Takahashi, M. (2012). Semi-Active Suspension Control Considering Lateral Vehicle Dynamics Due to Road Input. *New Advances in Vehicular Technology and Auto-motive Engineering*, IntechOpen. http://dx.doi.org/10.5772/45789

Torbic, D. J., Harwood, D. W., Gilmore, D. K., Pfefer, R., Neuman, T. R., Slack, K. L., & Hardy, K. K. (2004). *Guidance for Implementation of the AASHTO Strategic Highway Safety Plan: A Guide for Reducing Collisions on Horizontal Curves*. NCHRP Report 500 Series, Transportation Research Board, Washington, D.C.

Vázquez, V. F., Hidalgo, M. E., García-Hoz, A. M., Camara, A., Terán F., Ruiz-Teran, A. M., & Paje, S. E. (2020). Tire/road noise, texture, and vertical accelerations: Surface assessment of an urban road. *Applied Acoustics*, *160*, 107153. https://doi.org/10.1016/j.apacoust.2019.107153

Vidas Žuraulis,
Vytenis Surblys

Assessment
of Risky Cornering
on a Horizontal Road
Curve by Improving
Vehicle Suspension
Performance

World Health Organization. (2018). *Global status report on road safety 2018*.

World Health Organization. (2020). *Road traffic injuries* https://www.who.int/news-room/fact-sheets/detail/road-traffic-injuries (Online Accessed 23 November 2020)

Xu, C., Wang, C., Ding, Y., & Wang, W. (2020) Investigation of extremely severe traffic crashes using fault tree analysis. *Transportation Letters*, *12*(3), 149–156. https://doi.org/10.1080/19427867.2018.1540146

Xu, J., Luo, X. & Shao, YM. (2018). Vehicle trajectory at curved sections of two-lane mountain roads: a field study under natural driving conditions. *European Transport Research Review*, *10*, Article 12.
https://doi.org/10.1007/s12544-018-0284-x

Praticò, H., Kita, H., Xing, J., & Hirai, Sh. (2017). A car-accident rate index for curved roads: A speed choice–based approach. *Transportation Research Procedia*, *25*, 2108–2118. https://doi.org/10.1016/j.trpro.2017.05.404

Zhang, Y., Chen, W., Chen, L., & Shangguan, W. (2007). Non-stationary Random Vibration Analysis of Vehicle with Fractional Damping. *13th National Conference on Mechanisms and Machines*, 171–178.

Yang, J., Ning, D., Sun, S. S., Zheng, J., Lu, H., Nakano, M., Zhang, S., Du, H., & Li, W. H. (2021). A semi-active suspension using a magnetorheological damper with non-linear negative-stiffness component. *Mechanical Systems and Signal Processing*, 147, 107071. https://doi.org/10.1016/j.ymssp.2020.107071

Yang, S., Li, S., Chen, L. (2015). *Dynamics of Vehicle–Road Coupled System*. Springer.

Žuraulis, V., & Sokolovskij, E. (2015). Vehicle Velocity Relation to Slipping Trajectory Change: An Option for Traffic Accident Reconstruction. *Promet – Traffic & Transportation*, *30*(4), 395–406.
https://doi.org/10.7307/ptt.v30i4.2720

Žuraulis, V., Sokolovskij, E., & Matijošius, J. (2015). The opportunities for establishing the critical speed of the vehicle on research in its lateral dynamics. *Eksploatacja i Niezawodnosc – Maintenance and Reliability*, *15*(4), 312–318.

Žuraulis, V., Surblys, V., & Šabanovič, E. (2019). Technological measures of forefront road identification for vehicle comfort and safety improvement. *Transport*, *34*(3), 363–372. https://doi.org/10.3846/transport.2019.10372

12th Annual Road Safety Performance Index (PIN) Report. (2018). *European Transport Safety Council*. https://etsc.eu/12th-annual-road-safety-performance-index-pin-report/